

1 Using a Network of Locally Developed Low Cost Particulate  
2 Matter Sensors for Land Use Regression Modeling of PM<sub>2.5</sub>  
3 in Urban Uganda

4

5

6 Eric S. Coker<sup>1\*</sup>, Joel Ssematimba<sup>2</sup>, Engineer Bainomugisha<sup>2</sup>

7

8 <sup>1</sup>Department of Environmental and Global Health, College of Public Health and Health,

9 Professions, University of Florida, 1255 Center Dr., Gainesville, FL.; eric.coker@php.ufl.edu

10 <sup>2</sup>AirQo, Department of Computer Science, College of Computing and Information Sciences,

11 Makerere University, Plot 56 Pool Road, Kampala, Uganda.

12

13 \*Corresponding Author

14

## 15 **Acknowledgements**

16

17 We would like to acknowledge the tireless efforts of the AirQo staff who assisted with data

18 collection and data management.

19

20

21

22

## 23 **ABSTRACT**

24

### 25 **Background**

26

27 There are major air pollution monitoring gaps in sub-Saharan Africa. Developing capacity in the  
28 region to conduct air monitoring in the region can help estimate exposure to air pollution for  
29 epidemiology research. The purpose of our study is to develop a land use regression (LUR)  
30 model using low-cost air quality sensors developed by a research group in Uganda (AirQo).

31

### 32 **Methods**

33

34 Using these low-cost sensors, we collected continuous measurements of fine particulate matter  
35 (PM<sub>2.5</sub>) between May 1, 2019 and February 29, 2020 at 22 monitoring sites across urban  
36 municipalities of Uganda. We compared average monthly PM<sub>2.5</sub> concentrations from the AirQo  
37 sensors with measurements from a BAM-1020 reference monitor operated at the US Embassy in  
38 Kampala. Monthly PM<sub>2.5</sub> concentrations were used for LUR modeling. We used eight Machine  
39 Learning (ML) algorithms and ensemble modeling; using 10-fold cross validation and root mean  
40 squared error (RMSE) to evaluate model performance.

41

### 42 **Results**

43

44 Monthly PM<sub>2.5</sub> concentration was 60.2  $\mu\text{g}/\text{m}^3$  (IQR: 45.4-73.0  $\mu\text{g}/\text{m}^3$ ; median= 57.5  $\mu\text{g}/\text{m}^3$ ). For  
45 the ML LUR models, RMSE values ranged between 5.43  $\mu\text{g}/\text{m}^3$  - 15.43  $\mu\text{g}/\text{m}^3$  and explained

46 between 28% and 92% of monthly PM<sub>2.5</sub> variability. Generalized additive models explained the  
47 largest amount of PM<sub>2.5</sub> variability ( $R^2=0.92$ ) and produced the lowest RMSE ( $5.43 \mu\text{g}/\text{m}^3$ ) in  
48 the held-out test set. The most important predictors of monthly PM<sub>2.5</sub> concentrations included  
49 monthly precipitation, major roadway density, population density, latitude, greenness, and  
50 percentage of households using solid fuels.

51

## 52 **Conclusion**

53

54 To our knowledge, ours is the first study to model the spatial distribution of urban air pollution in  
55 sub-Saharan Africa using air monitors developed from the region itself. Non-parametric ML for  
56 LUR modeling performed with high accuracy for prediction of monthly PM<sub>2.5</sub> levels. Our  
57 analysis suggests that locally produced low-cost air quality sensors can help build capacity to  
58 conduct air pollution epidemiology research in the region.

59

## 60 **KEYWORDS**

61 land use regression, low-cost sensors, machine learning, particulate matter, Africa

62

## 63 **1. Introduction**

64

65 Data gaps in lower and middle-income countries (LMICs) related to environmental pollution is  
66 limiting environmental policy development and governance as well as our understanding of  
67 health impacts from pollution in LMICs. Low-cost sensors (LCS) hold great promise for being  
68 able to bridge these environmental pollution data gaps in LMICs. (Amegah, 2018) The

69 widespread use of LCSs in LMIC settings, however, is yet to be realized. This underutilization of  
70 LCS in LMICs is due to both technical and non-technical reasons, including: (1) limitations of  
71 data quality collected by LCSs; (2) a lack of downstream data analytics applications for LCSs;  
72 and (3) a lack of consideration for sustainable operating mechanisms and physical and  
73 socioeconomic contexts in LMICs.(Amegah, 2018; Mao et al., 2019) Despite their current  
74 limitations, low-cost air quality sensors (LCAQS) have made substantial progress in terms of  
75 acceptance for their use in certain air pollution measurement and research applications.

76 (Amegah, 2018; Clements et al., 2017; Malings et al., 2020; Masiol et al., 2019, 2018;  
77 McKercher and Vanos, 2018; Weissert et al., 2020, 2019)

78  
79 Emergent LCAQS applications include the capability to enhance air quality regulatory  
80 monitoring by improving spatial and temporal resolution of current air monitoring programs,  
81 (Malings et al., 2020; McKercher and Vanos, 2018) and identifying particulate matter (PM)  
82 sources in complex urban environments. (Hagan et al., 2019) Recent studies conducted in the  
83 U.S. suggest that air pollution data collected using LCAQS can also help with generating spatio-  
84 temporal models that can reliably predict fine spatial-scale urban air pollution concentrations.  
85 (Masiol et al., 2019, 2018; Weissert et al., 2020, 2019) The present study builds off of these  
86 recent advances in air pollution-modeling by using LCAQS data for a spatial air pollution-  
87 prediction model. Where our study differs, however, is we implement the study in the LMIC  
88 context of urban Uganda.

89  
90 What makes our study particularly unique is that we are using a spatially dense network of  
91 LCAQS that have been designed and fabricated locally in Uganda. These LCAQS developed by

92 AirQo are the first, to our knowledge, to originate from a sub-Saharan Africa (SSA) country.  
93 Such locally designed and produced LCAQS can plausibly address several limitations of other  
94 LCAQS, including offering a more sustainable operating mechanism as well as creating an  
95 LCAQS designed to operate in the challenging urban SSA infrastructural, socioeconomic and  
96 environmental context. For instance, the LCAQS used in our study, named AirQo, are designed  
97 and optimized to work in places characterized by sporadic internet connectivity, irregular power  
98 supply, high temperatures and dusty environments. The devices include a custom designed  
99 filtration system to minimize clogging, dust deposition, and reduce insect infestation common in  
100 the SSA region. Therefore, this study is motivated by a proof-of-concept in terms of using  
101 locally-sourced LCAQS for developing a LUR model to be employed in future ambient air  
102 pollution epidemiology research in the SSA region.

103  
104 Moreover, conventional LUR air pollution modeling is implemented using multivariable linear  
105 regression and often applies K-fold cross-validation to validate the prediction model. (Brokamp  
106 et al., 2017; Eeftens et al., 2012; Mao et al., 2012; Sahsuvaroglu et al., 2006) Recent advances in  
107 LUR air pollution modeling suggests that Machine Learning (ML) algorithms, such as Random  
108 Forests (RF), helps deal with overfitting and relaxing assumptions of linearity. (Araki et al.,  
109 2018; Beckerman et al., 2013; Brokamp et al., 2017; Di et al., 2019; Rahman et al., 2020;  
110 Weissert et al., 2020, 2019) Hence, our study takes a ML approach to LUR modeling, using the  
111 data generated from the LCAQS network described in this study.

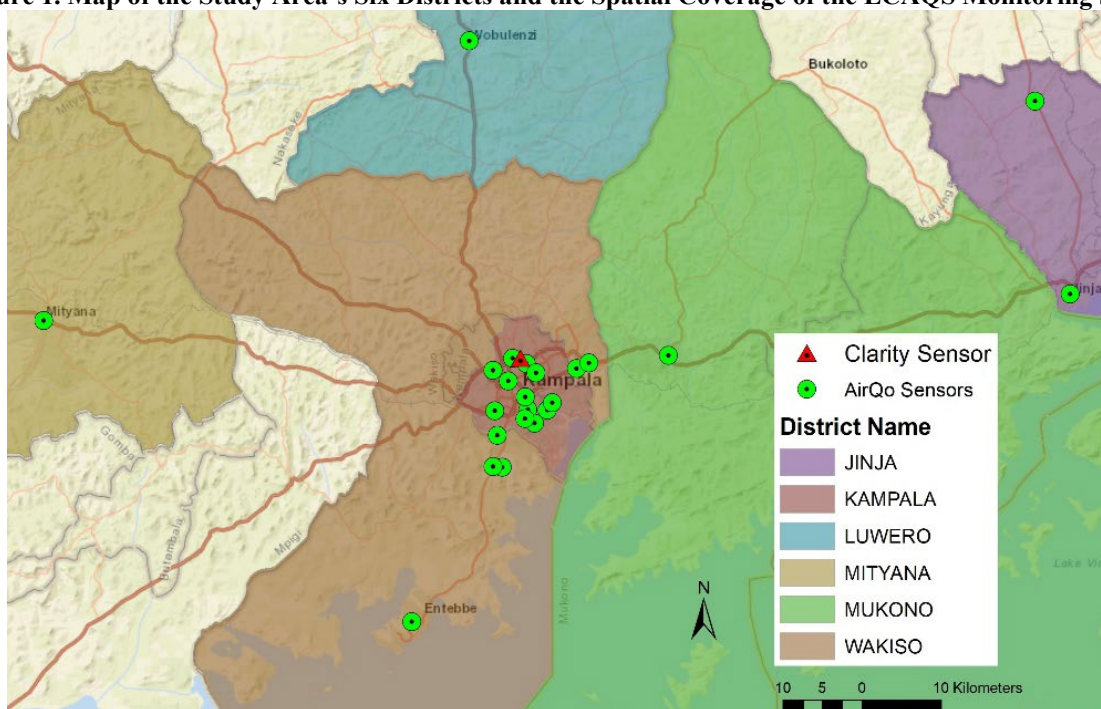
112

## 113 **2. Materials and Methods**

114

115 The country of Uganda straddles the equator and is located in the East Africa region of SSA. The  
116 study area (Figure 1) encompasses six urban sites of Uganda's central and eastern region,  
117 including Jinja, Kampala, Luwero, Mityana, Mukono, and Wakiso districts. Uganda's capital  
118 city, Kampala, where nearly two-thirds (n=14) of the LCAQS were placed in our study, is  
119 located along the northern shores of Lake Victoria at an altitude of approximately 1,140 meters  
120 above sea level. (Fuhriemann et al., 2015) The districts included in the study have a wide range of  
121 population sizes; ranging from ~2.0 million, 1.5 million, 0.6 million, 0.47 million, 0.46 million,  
122 and 0.33 million, for Wakiso, Kampala, Mukono, Jinja, Luwero, and Mityana, respectively.  
123 (UBOS, 2014)

124 **Figure 1. Map of the Study Area's Six Districts and the Spatial Coverage of the LCAQS Monitoring Sites.**



125  
126

127

## 128 **2.2. PM2.5 Measurements**

### 129 *2.2.1. Sensor Network*

130 The AirQo devices measure particulate matter (PM) PM2.5 and PM10 using a nephelometer  
131 (light-scattering) technology. The devices also measure location (latitude, longitude) and  
132 meteorology parameters including internal and external temperature, atmospheric pressure, and  
133 humidity. The AirQo devices transmit data over a local Global System for Mobile  
134 Communications (GSM) network every 90 seconds and can run off solar or mains. Currently, we  
135 have deployed devices at static locations and mobile monitors (e.g., motorcycle taxis) thereby  
136 forming a network of both fixed and dynamic nodes. Currently, the sensor network includes 65  
137 nodes with 40 in Kampala area and 25 in other urban areas of Uganda. In this study we use the  
138 data from the fixed monitoring locations only and have restricted the data to monitors that have  
139 been in operation for at least 75% of the study period (n=22 AirQo sensors). We installed  
140 devices between 2.5 and 4 meters high. Sensor placement is determined on a number of spatial  
141 features including population density, land use, road network, pollution sources and receptors,  
142 economic activities, and practical limitations, among others. The fixed installation locations  
143 include private property, schools, buildings, and lighting poles. Depending on the installation  
144 location, we fabricated custom mountings to support and secure the air quality monitor. To  
145 ensure data quality, at least one AirQo devices is co-located near (~10 meters) a Beta  
146 Attenuation Mass Monitor (BAM)1020 reference monitor currently installed and operated at the  
147 U.S. Embassy in Kampala. Additionally, for internal data quality assurance, each device includes  
148 two PM sensors. This dual sensor approach enables us to rapidly compare a given sensor against  
149 its twin sensor in order to detect any problems for the sensor. The collected data are transmitted  
150 in near real-time to a cloud-based platform. In addition to the AirQo sensors, we also used

151 another LCAQS known as Clarity Node (n=1). The Clarity sensor uses a similar nephelometer  
 152 technology that the AirQo device uses to detect PM<sub>2.5</sub>. Additionally, the Clarity sensor transmits  
 153 PM monitoring data over a local GSM network in near real-time to a cloud. (Pantelic et al.,  
 154 2019) The majority of the LCAQS used in this study are AirQo sensors (n=22) while only one  
 155 Clarity Node-S sensor was used.

156

## 157 2.3. PM<sub>2.5</sub> Estimation

### 158 2.3.1. Predictor Variables

159 We assembled 18 predictor variables for LUR modeling. We define these variables using four  
 160 broad categories, including spatial variables, meteorological variables, land use variables, and  
 161 demographic variables. Table 1 summarizes the relevant information for each of the predictor  
 162 variables in terms of their range of buffer sizes, spatial resolution, data format, and references.

163 **Table 1. Predictor Variables used for LUR Modeling.**

Variable	Buffer Size/Resolution/Spatial Unit	Data Format	Reference
<i>Meteorological and Spatial Predictors</i>			
Precipitation	Inches (monthly averages; 2005-2015)	Tabular/Vector	( <a href="https://www.timeanddate.com/weather/uganda/entebbe/climate">https://www.timeanddate.com/weather/uganda/entebbe/climate</a> , n.d.)
Latitude		Tabular/Vector	
Longitude		Tabular/Vector	
Elevation	100m	Raster values transformed into Vector for analysis	(USGS, n.d.)
<i>Land Use Predictors</i>			
Major Roadways	250m buffer	Raster values transformed into Vector for analysis	(OpenStreetMap, n.d.)
Major Roadways	500m buffer	Raster values transformed into	(OpenStreetMap, n.d.)



		Vector for analysis	
Major Roadways	750m buffer	Raster values transformed into Vector for analysis	(OpenStreetMap, n.d.)
Greenness (NDVI)	250m buffer/250m	Raster values transformed into Vector for analysis	(FEWSNET, n.d.)
Greenness (NDVI)	500m buffer/250m	Raster values transformed into Vector for analysis	(FEWSNET, n.d.)
Greenness (NDVI)	750m buffer/250m	Raster values transformed into Vector for analysis	(FEWSNET, n.d.)
<i>Demographic and Household Predictors</i>			
Number of People	Parish-level	Tabular/Vector	(UBOS, n.d.)
Number of Households	Parish-level	Tabular/Vector	(UBOS, n.d.)
Household Density (number of households/Parish area)	Parish-level	Raster values transformed into Vector for analysis	(UBOS, n.d.)
Percent Households Solid Fuel Use	Parish-level	Tabular/Vector	(UBOS, n.d.)
Population Density	~2km	Tabular/Vector	(HDX, n.d.)
Population Density	250m buffer/~2km	Tabular/Vector	(HDX, n.d.)
Population Density	500m buffer/~2km	Tabular/Vector	(HDX, n.d.)
Population Density	750m buffer/~2km	Tabular/Vector	(HDX, n.d.)

164

### 165 2.3.2. Statistical Analysis and Land Use Regression Modeling

166 We used PM<sub>2.5</sub> concentration data from 23 LCAQS in total, including 22 sensors from the  
167 AirQo network and one Clarity sensor. We used sensor data collected between May 1, 2019 and  
168 February 29, 2020. Monthly PM<sub>2.5</sub> air concentration averages were computed (n=218  
169 observations) and combined with covariates for the LUR modeling. We calculated summary  
170 statistics for the monthly averages overall for the study area and stratified by month and district.

171 We then calculated Pearson correlation coefficients between monthly PM2.5 averages and land  
172 use variables. Since the distribution of monthly averaged PM2.5 measurements were highly  
173 right-skewed, we log-transformed PM2.5 concentrations for the machine learning LUR (ML-  
174 LUR) modeling described in turn. We used monthly PM2.5 averages for modeling since the  
175 intended purpose of these exposure estimates is for predicting trimester-specific and entire  
176 pregnancy PM2.5 exposure averages for a future birth cohort study, as has been done in previous  
177 studies. (Coker et al., 2015)

178  
179 For the ML-LUR algorithms, the combined PM2.5 and LUR dataset was first split into a training  
180 set (90%) and validation test set (10%). Next, we performed 10-fold cross-validation on the  
181 training set (n=198 observations) only, using root mean squared error (RMSE) to guide each  
182 base learner model. Eight different ML algorithms were fit in order to compare each learner's  
183 performance. These models include linear regression model (LM), Support Vector Machines  
184 with Radial Basis Function Kernel (SVM), Random Forest (RF), Quantile Random Forest  
185 (QRF), eXtreme Gradient Boosting (xgbTree), Generalized Additive Model (GAM), Lasso and  
186 Elastic-Net Regularized Generalized Linear Models (GLMNET), and Least Angle Regression  
187 (LARS). All 18 covariates described in Table 1, which included land use variables (e.g., major  
188 roadway density, greenspace), population demographic variables, and historical precipitation  
189 data, were included in the analysis. We implemented the base ML algorithms using the *caret*  
190 package in R, with the '*caretList*' command used to fit all ML algorithms in parallel. In addition  
191 to the individual base learner models already mentioned, we performed ensemble modeling using  
192 the *caret* package in order to assess whether improved ML-LUR model performance is achieved  
193 through ensemble modeling as seen in (Di et al., 2019 and Lim et al., 2019). (Di et al., 2019; Lim

194 et al., 2019) We implemented ensemble modeling with the *caretEnsemble* package in R, using  
195 approaches offered by the ‘*caretEnsemble*’ (CE) and ‘*caretStack*’ (CS) commands. For the CE  
196 approach, we applied GLM to create a linear combination of all base learner models. Whereas in  
197 the CS approach we applied a stacked caret approach that combined the results from multiple  
198 component caret models. Since there were strong correlations between results from the base  
199 learner models, we used GLMNET when applying the stacked approach. Our final assessment of  
200 RMSE and  $R^2$  applied to the 10% held-out test set only since this should better represent the  
201 ability of the ML-LUR to predict monthly PM2.5 concentrations at unmeasured locations for our  
202 study area.

### 203 **3. RESULTS**

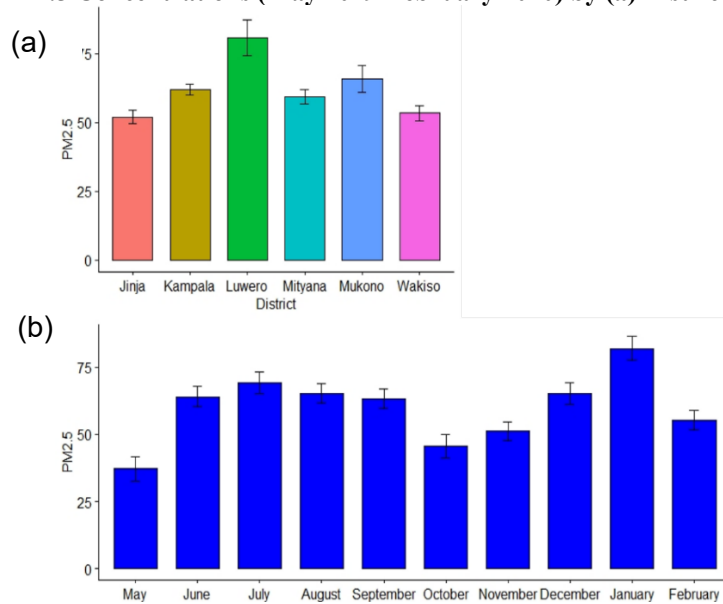
#### 204 **3.1. PM2.5 Monitoring Results**

205 Average monthly PM2.5 concentrations for the entire study area was  $60.2 \mu\text{g}/\text{m}^3$  (IQR: 45.4-73.0  
206  $\mu\text{g}/\text{m}^3$ ; median=  $57.5 \mu\text{g}/\text{m}^3$ ). According to Figure 2a, monitoring sites in Luwero and Mukono  
207 Districts exhibited the highest PM2.5 levels. As expected, according to Figure 2b, elevated  
208 PM2.5 concentrations were observed to be lowest during the wet season and highest during the  
209 dry season.

##### 210 **3.1.1. Comparison of AirQo with a reference monitor**

211 For comparison, we co-located an AirQo sensor with a BAM1020 reference monitor located at  
212 the US Embassy in Kampala. The mean monthly PM2.5 concentrations were  $63.1 \mu\text{g}/\text{m}^3$  and  
213  $60.2 \mu\text{g}/\text{m}^3$  for the BAM1020 and AirQo monitors, respectively. Figure 3 plots the monthly  
214 PM2.5 averages of the BAM1020 embassy monitor versus the AirQo sensor. With an RMSE of  
215  $5.58 \mu\text{g}/\text{m}^3$ , normalized RMSE of 8.8%, and an  $R^2$  of 0.87, the AirQo sensor compare well with  
216 the BAM1020 in terms of monthly averages.

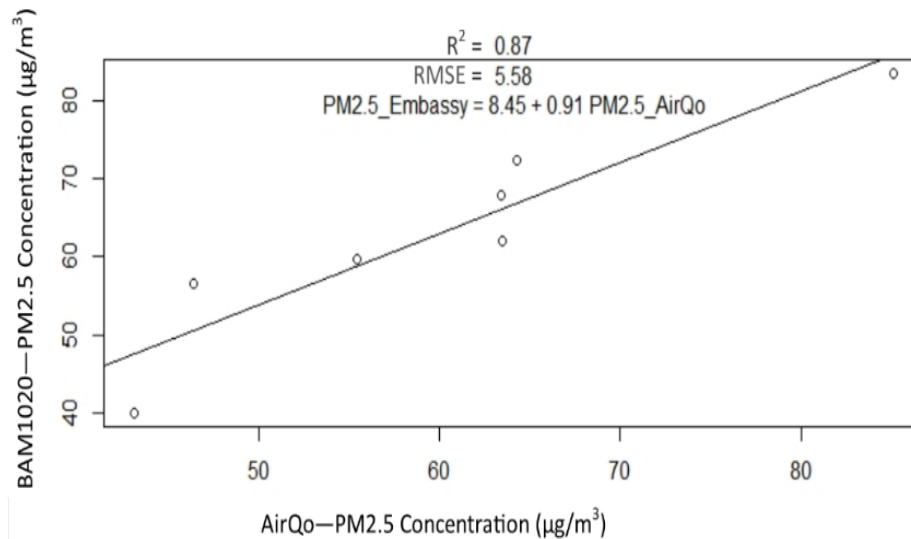
217

**Figure 2. PM<sub>2.5</sub> Concentrations (May 2019-February 2020) by (a) District and (b) Month.**

218

219

220

**Figure 3. Average Monthly PM<sub>2.5</sub> Concentrations from AirQo and BAM1020 Monitors.**

221

222

### 223 3.2. ML-LUR Results

224 We summarize the RMSE and  $R^2$  values for the base learner models and ensemble models in  
 225 Table 2 (for log-transformed and exponentiated values). These values were computed using the  
 226 held-out test set (N=20) only. The GAM resulted in the lowest RMSE as well as highest  $R^2$   
 227 values ( $R^2=0.94$ ) for the log-transformed values. Even the ensemble models performed quite

228 well, as shown in Table 2, both the GAM and xgbTree models outperformed the ensemble  
 229 models. The exponentiated predictions exhibit a similar pattern as the log-transformed values,  
 230 indicating the GAM with the lowest RMSE (5.43  $\mu\text{g}/\text{m}^3$ ) and highest  $R^2$  (0.92) values.

231 **Table 2. Performance (RMSE and  $R^2$ ) for Models**

Model	RMSE <sup>a</sup>	$R^2$ <sup>a</sup>	RMSE <sup>b</sup>	$R^2$ <sup>b</sup>
GAM	0.083	0.94	5.43	0.92
xgbTree	0.111	0.87	6.75	0.85
Stacked Ensemble (glmnet)	0.117	0.85	7.10	0.84
Ensemble (lm)	0.121	0.83	7.35	0.83
RF	0.148	0.81	7.60	0.82
QRF	0.183	0.70	9.62	0.69
SVM	0.195	0.54	12.6	0.45
LM	0.198	0.54	13.2	0.42
LARS	0.210	0.50	13.9	0.39
GLMNET	0.242	0.37	15.4	0.28

232 <sup>a</sup>Log-transformed (not exponentiated)

233 <sup>b</sup>Exponentiated

234

### 235 3.2.1. Variable Importance

236 As shown in Figure A1 in the Appendix, several of the LUR variables are moderately to highly  
 237 correlated with one another. After extracting the variable importance values of study variables,  
 238 as calculated from the top performing model (GAM), we are able to rank the ML-LUR variables  
 239 in terms of predicting monthly PM2.5 concentrations. According to Figure A2, precipitation,  
 240 greenness (NDVI), roadway density, latitude, and solid fuel usage are the top-ranking variables.  
 241 When restricting our analysis to the top-5 predictor categories (precipitation, NDVI, roadway  
 242 density, latitude, and solid fuel use) only, the GAM model explained 88% of the monthly PM2.5  
 243 concentration variability using the entire data set (data not shown).

## 244 **Discussion**

245 In our study, we leveraged air quality data from a network of mostly locally designed and  
246 produced LCAQS that were then used to predict estimates of PM<sub>2.5</sub> in urban districts of Uganda.  
247 Moreover, we applied ML to optimize the LUR model. Importantly, we find that the AirQo  
248 sensors compare well against a BAM1020 reference monitor co-located at the U.S. Embassy. In  
249 general, when using predictors typically used in LUR modeling, the non-parametric ML  
250 algorithms performed the best in terms of being able to accurately predict monthly PM<sub>2.5</sub>  
251 concentrations when compared to parametric modeling (e.g., linear model).

252  
253 Of the land use predictors considered in our study, several stood out as strong predictors. The  
254 strongest predictors include precipitation, greenness, density of major roadways, latitude, solid  
255 fuel usage, and population density. To our knowledge, our study is the first to use population  
256 census data on solid fuel usage (at the Parish-level) in a LUR model. Specifically, we find that  
257 higher solid fuel usage is positively correlated with monthly PM<sub>2.5</sub> concentrations. This finding  
258 suggests that area-level solid fuel use data can help inform LUR prediction models for PM<sub>2.5</sub> in  
259 lower income SSA urban areas, and potentially other regions with high levels of solid fuel usage.  
260 Previous LUR prediction models for PM<sub>2.5</sub> in SSA have been shown to have relatively poorer  
261 performance(Saucy et al., 2018; Tularam, 2019) compared to gaseous pollutant models for SSA  
262 or PM<sub>2.5</sub> models developed in higher income regions. Given our results, as well as other air  
263 pollution research conducted in urban SSA that also show strong correlations between  
264 neighborhood-level solid fuel use and outdoor PM concentrations(Zhou et al., 2011), we suggest  
265 future modeling efforts in this region should incorporate solid fuel use data to improve PM<sub>2.5</sub>  
266 modeling predictions.

267  
268 To our knowledge, this is the first study to use LCAQS for LUR modeling in SSA. As suggested  
269 by previous authors(Amegah, 2018), we demonstrate that LCAQS hold strong potential for  
270 providing highly spatially resolved PM<sub>2.5</sub> measurement data that can be harnessed for exposure  
271 estimation in air pollution epidemiology research. While data can be integrated to improve model  
272 performance, such as aerosol optical depth (AOD) remote sensing data, we are encouraged by  
273 our findings. Future analyses will focus on optimizing calibration approaches for the AirQo PM  
274 sensor data. Since accurate measurement of PM<sub>2.5</sub> with light scattering sensors can be limited by  
275 accuracy errors caused by environmental parameters such as relative humidity and temperature  
276 and may be subject to drift(US EPA, n.d.), we will use a co-located reference method (e.g.,  
277 BAM1020) and model the influence of relative humidity (RH) and temperature on measurement  
278 accuracy; which can then be used in turn for regression-based calibration purposes in future  
279 epidemiology research. (Wang et al., 2019)

280

## 281 **Conclusion**

282 Deploying LCAQS can help address the urgent and growing need for expanding and improving  
283 air quality monitoring in resource-limited settings of SSA. With reasonably accurate predictions  
284 of PM<sub>2.5</sub> using ML-LUR with 10-fold cross-validation, data from the locally developed AirQo  
285 sensors used in the present study provided evidence suggesting that they can be used for  
286 modeling exposures for a birth cohort study.

287

## 288 **References**

- 289 Amegah, A.K., 2018. Proliferation of low-cost sensors. What prospects for air  
290 pollution epidemiologic research in Sub-Saharan Africa? *Environ. Pollut.*  
291 241, 1132–1137. <https://doi.org/10.1016/j.envpol.2018.06.044>
- 292 Araki, S., Shima, M., Yamamoto, K., 2018. Spatiotemporal land use random forest  
293 model for estimating metropolitan NO<sub>2</sub> exposure in Japan. *Sci. Total*  
294 *Environ.* 634, 1269–1277. <https://doi.org/10.1016/j.scitotenv.2018.03.324>
- 295 Beckerman, B.S., Jerrett, M., Martin, R.V., van Donkelaar, A., Ross, Z., Burnett,  
296 R.T., 2013. Application of the deletion/substitution/addition algorithm to  
297 selecting land use regression models for interpolating air pollution  
298 measurements in California. *Atmos. Environ.* 77, 172–177.  
299 <https://doi.org/10.1016/j.atmosenv.2013.04.024>
- 300 Brokamp, C., Jandarov, R., Rao, M.B., LeMasters, G., Ryan, P., 2017. Exposure  
301 assessment models for elemental components of particulate matter in an  
302 urban environment: A comparison of regression and random forest  
303 approaches. *Atmos. Environ.* 151, 1–11.  
304 <https://doi.org/10.1016/j.atmosenv.2016.11.066>
- 305 Clements, A.L., Griswold, W.G., Rs, A., Johnston, J.E., Herting, M.M., Thorson,  
306 J., Collier-Oxandale, A., Hannigan, M., 2017. Low-Cost Air Quality  
307 Monitoring Tools: From Research to Practice (A Workshop Summary).  
308 *Sensors* 17, 2478. <https://doi.org/10.3390/s17112478>



309 Coker, E., Ghosh, J., Jerrett, M., Gomez-Rubio, V., Beckerman, B., Cockburn, M.,  
310 Liverani, S., Su, J., Li, A., Kile, M.L., Ritz, B., Molitor, J., 2015. Modeling  
311 spatial effects of PM<sub>2.5</sub> on term low birth weight in Los Angeles County.  
312 Environ. Res. 142, 354–364. <https://doi.org/10.1016/j.envres.2015.06.044>

313 Di, Q., Amini, H., Shi, L., Kloog, I., Silvern, R., Kelly, J., Sabath, M.B., Choirat,  
314 C., Koutrakis, P., Lyapustin, A., Wang, Y., Mickley, L.J., Schwartz, J.,  
315 2019. An ensemble-based model of PM<sub>2.5</sub> concentration across the  
316 contiguous United States with high spatiotemporal resolution. Environ. Int.  
317 130, 104909. <https://doi.org/10.1016/j.envint.2019.104909>

318 Eeftens, M., Beelen, R., de Hoogh, K., Bellander, T., Cesaroni, G., Cirach, M.,  
319 Declercq, C., Dèdelè, A., Dons, E., de Nazelle, A., Dimakopoulou, K.,  
320 Eriksen, K., Falq, G., Fischer, P., Galassi, C., Gražulevičienė, R., Heinrich,  
321 J., Hoffmann, B., Jerrett, M., Keidel, D., Korek, M., Lanki, T., Lindley, S.,  
322 Madsen, C., Mölter, A., Nádor, G., Nieuwenhuijsen, M., Nonnemacher, M.,  
323 Pedeli, X., Raaschou-Nielsen, O., Patelarou, E., Quass, U., Ranzi, A.,  
324 Schindler, C., Stempfelet, M., Stephanou, E., Sugiri, D., Tsai, M.-Y., Yli-  
325 Tuomi, T., Varró, M.J., Vienneau, D., Klot, S. von, Wolf, K., Brunekreef,  
326 B., Hoek, G., 2012. Development of Land Use Regression Models for PM<sub>2.5</sub>  
327 , PM<sub>2.5</sub> Absorbance, PM<sub>10</sub> and PM<sub>coarse</sub> in 20 European Study Areas;

- 328 Results of the ESCAPE Project. *Environ. Sci. Technol.* 46, 11195–11205.  
329 <https://doi.org/10.1021/es301948k>
- 330 FEWSNET, n.d. Products | Early Warning and Environmental Monitoring Program  
331 [WWW Document]. URL <https://earlywarning.usgs.gov/fews/product/448>  
332 (accessed 2.24.20).
- 333 Fuhrmann, S., Stalder, M., Winkler, M.S., Niwagaba, C.B., Babu, M., Masaba, G.,  
334 Kabatereine, N.B., Halage, A.A., Schneeberger, P.H.H., Utzinger, J., Cissé,  
335 G., 2015. Microbial and chemical contamination of water, sediment and soil  
336 in the Nakivubo wetland area in Kampala, Uganda. *Environ. Monit. Assess.*  
337 187, 475. <https://doi.org/10.1007/s10661-015-4689-x>
- 338 Hagan, D.H., Gani, S., Bhandari, S., Patel, K., Habib, G., Apte, J.S., Hildebrandt  
339 Ruiz, L., Kroll, J.H., 2019. Inferring Aerosol Sources from Low-Cost Air  
340 Quality Sensor Measurements: A Case Study in Delhi, India. *Environ. Sci.*  
341 *Technol. Lett.* 6, 467–472. <https://doi.org/10.1021/acs.estlett.9b00393>
- 342 HDX, n.d. High Resolution Population Density Maps - Humanitarian Data  
343 Exchange [WWW Document]. URL  
344 <https://data.humdata.org/dataset/highresolutionpopulationdensitymaps>  
345 (accessed 2.24.20).
- 346 <https://www.timeanddate.com/weather/uganda/entebbe/climate>, n.d. Climate &  
347 Weather Averages in Entebbe, Uganda [WWW Document]. URL

- 348 <https://www.timeanddate.com/weather/uganda/entebbe/climate> (accessed  
349 2.24.20).
- 350 Lim, C.C., Kim, H., Vilcassim, M.J.R., Thurston, G.D., Gordon, T., Chen, L.-C.,  
351 Lee, K., Heimbinder, M., Kim, S.-Y., 2019. Mapping urban air quality using  
352 mobile sampling with low-cost sensors and machine learning in Seoul, South  
353 Korea. *Environ. Int.* 131, 105022.  
354 <https://doi.org/10.1016/j.envint.2019.105022>
- 355 Malings, C., Tanzer, R., Hauryliuk, A., Saha, P.K., Robinson, A.L., Presto, A.A.,  
356 Subramanian, R., 2020. Fine particle mass monitoring with low-cost  
357 sensors: Corrections and long-term performance evaluation. *Aerosol Sci.*  
358 *Technol.* 54, 160–174. <https://doi.org/10.1080/02786826.2019.1623863>
- 359 Mao, F., Khamis, K., Krause, S., Clark, J., Hannah, D.M., 2019. Low-Cost  
360 Environmental Sensor Networks: Recent Advances and Future Directions.  
361 *Front. Earth Sci.* 7, 221. <https://doi.org/10.3389/feart.2019.00221>
- 362 Mao, L., Qiu, Y., Kusano, C., Xu, X., 2012. Predicting regional space–time  
363 variation of PM<sub>2.5</sub> with land-use regression model and MODIS data.  
364 *Environ. Sci. Pollut. Res.* 19, 128–138. [https://doi.org/10.1007/s11356-011-](https://doi.org/10.1007/s11356-011-0546-9)  
365 0546-9
- 366 Masiol, M., Squizzato, S., Chalupa, D., Rich, D.Q., Hopke, P.K., 2019. Spatial-  
367 temporal variations of summertime ozone concentrations across a

- 368 metropolitan area using a network of low-cost monitors to develop 24 hourly  
369 land-use regression models. *Sci. Total Environ.* 654, 1167–1178.  
370 <https://doi.org/10.1016/j.scitotenv.2018.11.111>
- 371 Masiol, M., Zíková, N., Chalupa, D.C., Rich, D.Q., Ferro, A.R., Hopke, P.K.,  
372 2018. Hourly land-use regression models based on low-cost PM monitor  
373 data. *Environ. Res.* 167, 7–14. <https://doi.org/10.1016/j.envres.2018.06.052>
- 374 McKercher, G.R., Vanos, J.K., 2018. Low-cost mobile air pollution monitoring in  
375 urban environments: a pilot study in Lubbock, Texas. *Environ. Technol.* 39,  
376 1505–1514. <https://doi.org/10.1080/09593330.2017.1332106>
- 377 OpenStreetMap, n.d. OpenStreetMap [WWW Document]. OpenStreetMap. URL  
378 <https://www.openstreetmap.org/> (accessed 2.24.20).
- 379 Pantelic, J., Dawe, M., Licina, D., 2019. Use of IoT sensing and occupant surveys  
380 for determining the resilience of buildings to forest fire generated PM2.5.  
381 *PLOS ONE* 14, e0223136. <https://doi.org/10.1371/journal.pone.0223136>
- 382 Rahman, M.M., Karunasinghe, J., Clifford, S., Knibbs, L.D., Morawska, L., 2020.  
383 New insights into the spatial distribution of particle number concentrations  
384 by applying non-parametric land use regression modelling. *Sci. Total*  
385 *Environ.* 702, 134708. <https://doi.org/10.1016/j.scitotenv.2019.134708>
- 386 Sahsuvaroglu, T., Arain, A., Kanaroglou, P., Finkelstein, N., Newbold, B., Jerrett,  
387 M., Beckerman, B., Brook, J., Finkelstein, M., Gilbert, N.L., 2006. A Land

388 Use Regression Model for Predicting Ambient Concentrations of Nitrogen  
389 Dioxide in Hamilton, Ontario, Canada. *J. Air Waste Manag. Assoc.* 56,  
390 1059–1069. <https://doi.org/10.1080/10473289.2006.10464542>

391 Saucy, A., Rösli, M., Künzli, N., Tsai, M.-Y., Sieber, C., Olaniyan, T., Baatjies,  
392 R., Jeebhay, M., Davey, M., Flückiger, B., Naidoo, R., Dalvie, M., Badpa,  
393 M., de Hoogh, K., 2018. Land Use Regression Modelling of Outdoor NO<sub>2</sub>  
394 and PM<sub>2.5</sub> Concentrations in Three Low Income Areas in the Western Cape  
395 Province, South Africa. *Int. J. Environ. Res. Public. Health* 15, 1452.  
396 <https://doi.org/10.3390/ijerph15071452>

397 Tularam, H., 2019. Land use Regression Model for Exposure Assessment in the  
398 Mace Birth Cohort Study in Ethekewini: *Environ. Epidemiol.* 3, 401.  
399 <https://doi.org/10.1097/01.EE9.0000610480.85058.4a>

400 UBOS, 2014. National Population and Housing Census. Kampala, UG.

401 UBOS, n.d. Visualizations – Uganda Bureau of Statistics. URL  
402 <https://www.ubos.org/data-portals-2/visualizations/> (accessed 2.24.20).

403 US EPA, n.d. *collocation\_instruction\_guide.pdf* [WWW Document]. URL  
404 [https://www.epa.gov/sites/production/files/2018-](https://www.epa.gov/sites/production/files/2018-01/documents/collocation_instruction_guide.pdf)  
405 [01/documents/collocation\\_instruction\\_guide.pdf](https://www.epa.gov/sites/production/files/2018-01/documents/collocation_instruction_guide.pdf) (accessed 5.12.20).

406 USGS, n.d. EarthExplorer - Home [WWW Document]. URL  
407 <https://earthexplorer.usgs.gov/> (accessed 2.24.20).

- 408 Wang, Y., Du, Y., Wang, J., Li, T., 2019. Calibration of a low-cost PM<sub>2.5</sub> monitor  
409 using a random forest model. *Environ. Int.* 133, 105161.  
410 <https://doi.org/10.1016/j.envint.2019.105161>
- 411 Weissert, L., Alberti, K., Miles, E., Miskell, G., Feenstra, B., Henshaw, G.S.,  
412 Papapostolou, V., Patel, H., Polidori, A., Salmond, J.A., Williams, D.E.,  
413 2020. Low-cost sensor networks and land-use regression: Interpolating  
414 nitrogen dioxide concentration at high temporal and spatial resolution in  
415 Southern California. *Atmos. Environ.* 223, 117287.  
416 <https://doi.org/10.1016/j.atmosenv.2020.117287>
- 417 Weissert, L.F., Alberti, K., Miskell, G., Pattinson, W., Salmond, J.A., Henshaw,  
418 G., Williams, D.E., 2019. Low-cost sensors and microscale land use  
419 regression: Data fusion to resolve air quality variations with high spatial and  
420 temporal resolution. *Atmos. Environ.* 213, 285–295.  
421 <https://doi.org/10.1016/j.atmosenv.2019.06.019>
- 422 Zhou, Z., Dionisio, K.L., Arku, R.E., Quaye, A., Hughes, A.F., Vallarino, J.,  
423 Spengler, J.D., Hill, A., Agyei-Mensah, S., Ezzati, M., 2011. Household and  
424 community poverty, biomass use, and air pollution in Accra, Ghana. *Proc.*  
425 *Natl. Acad. Sci.* 108, 11028–11033.  
426 <https://doi.org/10.1073/pnas.1019183108>
- 427

428

429

430

431

432

433

434